DEVELOPMENTAL BIOLOGY **187,** 224–235 (1997)
ARTICLE NO. DB978571

Inhibition of Morphogenetic Movement during *Xenopus* Gastrulation by Injected Sulfatase: and Dorsoventral Axis Formation

John B. Wallingford,*,[1] Amy K. Sater,† J. Akif Uzman,† and Michael V. Danilchik‡

**Department of Biology, Wesleyan University, Middletown, Connecticut 06459; †Department of Biology, University of Houston, Houston, Texas 77204; and ‡Department of Biological Structure and Function, Oregon Health Sciences University (SD), Portland, Oregon 97201-3097*

In order to explore the role of morphogenetic movement in the establishment of anteroposterior and dorsoventral axes, we sought to identify novel *in vivo* inhibitors of gastrulation movements in *Xenopus laevis*. Injection of hydrolytic sulfatase into the blastocoels of gastrula stage embryos resulted in severe anteroposterior truncation, without a corresponding truncation of the dorsoventral axis. Confocal microscopy of whole embryos revealed that gastrulation movements are severely disrupted by sulfatase; in addition, sulfatase dramatically inhibited chordomesodermal cell elongation and convergent extension movements in planar dorsal marginal zone explants. The phenotype of anteroposterior reduction elicited by sulfatase is distinctly different from commonly generated dorsoanterior phenotypes (e.g., ultraviolet irradiation of the vegetal cortex prior to cortical rotation or suramin injection), and the two varieties of phenotype appear to result from inhibition of distinct, separable components of the axis-generating machinery.

INTRODUCTION

Gastrulation of the frog *Xenopus laevis* is driven by several autonomous, region-specific morphogenetic processes (Keller, 1991). The timing and extent of these processes profoundly influence the outcome of larval patterning (reviewed in Slack *et al.*, 1992; Slack and Tannahill, 1992; Gerhart *et al.*, 1989). Previous studies have used explanted tissue from gastrulating embryos to investigate the mechanics of morphogenetic movement during gastrulation (Keller and Danilchik, 1988; Keller and Tibbetts, 1989; Winklbauer, 1990; Winklbauer and Nagel, 1991; Shih and Keller, 1992; Domingo and Keller, 1995, Moore *et al.*, 1995). In comparison, relatively little has been done to analyze gastrulation in experimentally manipulated whole embryos. Such *in vivo* experiments will be crucial to our understanding of how each of the morphogenetic processes of gastrulation contribute to the establishment of the vertebrate body axis.

[1] To whom correspondence should be addressed at Department of Zoology, University of Texas at Austin, Austin, TX 78712. Fax: 512-471-1188. E-mail: Wallingford@mail.utexas.edu.

In previous experiments, we inhibited gastrulation *in vivo* by injection of the polysulfonated compounds trypan blue and suramin. Blastocoelic injection of either of these compounds at progressively earlier stages resulted in progressive reduction of both anterior (e.g., cranial structures) and dorsal (e.g., neural tube and notochord) structures in *Xenopus* embryos (Gerhart *et al.*, 1989). This result suggested that proper morphogenetic movement during gastrulation is required for the establishment of both anteroposterior and dorsoventral axes. Indeed, many experimentally generated phenotypes involve both disruption of the morphogenetic movements of gastrulation and truncation of both dorsoventral and anteroposterior axes (Kao and Danilchik, 1991; Gerhart *et al.*, 1989).

In order to examine in whole embryos the relationship between gastrulation movements and larval pattern, we sought to identify novel *in vivo* inhibitors of morphogenetic movements during gastrulation. Given the well-recognized role of sulfated macromolecules in the early development of *Xenopus* (Waddington and Perry, 1956; Greenhouse and Hamburgh, 1968; Danilchik, 1986; Mitani, 1989, Kao and Danilchik, 1991, Brickman and Gerhart, 1994; Itoh and Sokol, 1994; Cardellini *et al.*, 1994), we injected hydrolytic

0012-1606/97 $25.00

sulfatase into the blastocoels of gastrulating *Xenopus* embryos and observed the effects using whole-mount confocal scanning laser microscopy (CSLM). Injected larvae exhibited dose- and stage-dependent truncation of anteroposterior character without corresponding truncation of dorsoventral character. We demonstrate that this truncation results from inhibition of morphogenetic movements during gastrulation, in particular, the migration of the head mesoderm, expansion of the archenteron, and convergent extension of the dorsal marginal zone. Determination of the molecular target(s) of sulfatase was beyond the scope of this investigation; rather, we sought to use sulfatase teratogenesis to determine the extent to which patterning of the anteroposterior and dorsoventral axes depends upon the morphogenetic movements of gastrulation.

We further explored the relationship between gastrulation and the establishment of both anteroposterior and dorsoventral axes by comparing the phenotypes generated by several treatments known to inhibit gastrulation, including injection of heparin, trypan blue, suramin, and sulfatase, as well as ultraviolet irradiation of the vegetal cortex prior to cortical rotation. From these comparisons, we suggest that a distinction be made between dorsoanterior reduction phenotypes and anteroposterior reduction phenotypes. Furthermore, we suggest that this distinction will be useful in relating larval phenotypes to events during early development.

MATERIALS AND METHODS

Embryos. Ovulation of female *X. laevis* was induced by injection of human chorionic gonadotropin. Eggs were fertilized *in vitro* and subsequently dejellied according to Peng (1991) and reared in MMR/3 at pH 7.2 at 15°C. Embryos were staged according to Nieuwkoop and Faber (1994).

Blastocoel injections. Sulfatase type H-5, type H-1, type IV, and type VIII; type IX-A β-glucuronidase, heparinase II, and chondroitinase ABC; and heparin, heparan sulfate, and chondroitin-5-sulfate sodium salts (Sigma) were dissolved in sterile, distilled water and centrifuged at 13k rpm to remove particulate matter. Trypan blue and suramin were prepared according to Kao and Danilchik (1991). All agents were injected to final concentrations noted in text or figure legends. Injections and ultraviolet irradiation were performed according to Kao and Danilchik (1991).

Assay of sulfatase activity. Sulfatase activity was assayed by spectrophotometric estimation of nitrocatechol liberated from p-nitrocatechol sulfate (pNCS) according to the procedure of Dodgson and Spencer (1957). Sulfatase type H-5 was dissolved in distilled water, and activity was assayed in a buffer of 2.5 m*M* pNCS (Sigma) and 0.25 *M* sodium acetate–acetic acid. Reactions proceeded at 37°C for 1 hr. Sodium hydroxide (1 *M*) was added to stop the reaction. Absorbance was then measured at 515 nm, and micrograms of nitrocatechol liberated/milliliter of enzyme solution/hour was calculated by $(A_t\text{-}A_c) \times 160.7$ (where A_t is the absorbance of the enzyme reaction mixture being tested and A_c is the absorbance of the no-enzyme control mixture).

Confocal microscopy. Embryos were fixed in Bouin's fixative at specified developmental stages. Picric acid was subsequently removed by extensive washing in 5 m*M* NH_4OH in 50% ethanol. Specimens were then placed in a solution of 15% hydrogen peroxide and 50% ethanol and bleached on a standard light box. After bleaching, embryos were devitellinated using sharpened watchmaker's forceps, dehydrated in an ethanol series, and cleared in 2:1::benzyl benzoate:benzyl alcohol (Dent and Klymkowsky, 1989). This fixation/bleaching protocol produced a strong autofluorescence of yolk platelets and bleached pigment granules, which was visualized with a Biorad MRC 500 confocal scanning laser microscope using a rhodamine (GHS) filter block.

Preparation and culture of explants. Explants of the dorsal marginal zone were prepared from embryos at stage 10+ as described (Sater *et al.*, 1993), except that the external epithelium was retained. For examination of convergence and extension, all explants were cut to a length of 1.18 mm. Explants were transferred to modified Danilchik's Medium (DFA; Sater *et al.*, 1993) with or without 100 units/ml H-5 sulfatase and placed interior side up beneath a fragment of anopore membrane (Nunc) supported with modeling clay. Anopore, an inorganic porous membrane used as a rigid support for cell or tissue cultures, was used to prevent healing of the explants and maintain planar configuration while allowing exposure of the tissue to the medium. Explants could easily be viewed through the anopore membrane, since it is transparent when wet. Sulfatase was added to culture medium immediately prior to use. Explant length was measured initially and again when intact control embryos reached stage 17. For measurements of cell elongation, explants were fixed at stage 17 in MEMFA (Harland, 1991), placed between two coverslips separated by modeling clay, and viewed with a Nikon CF 40× objective on a Nikon Diaphot microscope. Video images were taken with a Hamamatsu C-2400 CCD camera and analyzed using Optimas 4.02 image analysis software. In control explants, cells adjacent to the notochord–somite boundary were selected for measurement. In sulfatase-treated explants, cells located in the vegetalmost region of the mesoderm were selected for measurement, since cell elongation is initiated in this region.

Immunohistochemistry. Fixation and whole-mount immunohistochemistry were carried out as described in Hemmati-Brivanlou and Harland (1991). The monoclonal antibody Tor-70 was diluted 1:500 before use. The secondary antibody, peroxidase-conjugated rabbit anti-mouse IgG (Jackson Immunochemicals), was used at a 1:200 dilution and developed with diaminobenzidine. Where necessary, explants were bleached following immunohistochemistry, as described earlier. All antibody incubations were carried out overnight at 4°C. Video images were taken as described above.

RESULTS

Sulfatase Elicits Anteroposterior Defects

Injection of sulfatase into the blastocoels of gastrula stage *Xenopus* embryos resulted in marked reduction of cranial and anterior axial structures (Fig. 1). Lower doses of sulfatase produced varying degrees of cranial reduction (Figs. 1B and 1C), while higher doses elicited progressively more severe reduction of anterior axial structures as well as posterior structures, such as tail fin (Figs. 1D and 1E). Even in the most extremely affected individuals, some features of the anteroposterior axis always remained discernible (Fig. 1F). A pronounced ventral flexure of the anteroposterior axis was also a consistent feature of the phenotype (Figs. 1C–1F). In embryos receiving exceptionally high doses, blastopore closure occasionally failed. A simple index, the AnteroPost-

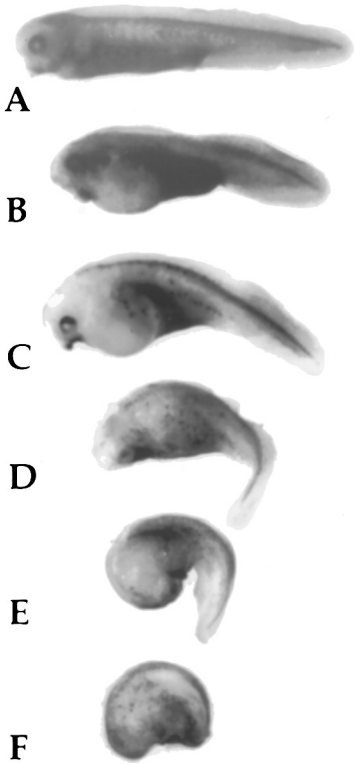

FIG. 1. The sulfatase-generated anteroposterior deficiency index, APDI (see also Table 1, A–F correspond to APDI = 5–0 respectively). Type IV sulfatase was injected into blastocoels at stage 9. The resulting phenotype is characterized at stage 40 by increasing reduction of cranial and axial structures along the anteroposterior axis and ventral flexure. Ventral flexure of the anteroposterior axis begins in the far anterior and is found more posteriorly in more severely affected individuals.

erior Deficiencies Index, or APDI, was designed to define degrees of severity of the sulfatase-generated phenotype (Table 1).

As shown in Fig. 2A, the sulfatase-generated phenotype proved to be dose-dependent, although a given dose often produced a wide range of phenotypes. Such variation has been observed in other blastocoel-injection experiments (Brickman and Gerhart, 1994) and is probably due to leakage of the reagent out of the blastocoel at the injection site (Kao and Danilchik, 1991). The severity of the phenotype was also dependent upon the stage of injection (Fig. 2B), with injections at the beginning of gastrulation resulting in more severe phenotypes and injections at later stages resulting in progressively less severe phenotypes. Injection of sulfatase as late as stage 12 resulted in distinct reduction of cranial structures and mild truncation of the anteroposterior axis. On the other hand, injection of heparinase II during gastrulation had no effect on larval pattern (data not shown; Brickman and Gerhart, 1994), indicating that the two enzymes affect embryogenesis via distinct mechanisms.

The various commercial preparations of sulfatase have varied levels of contaminating enzymes. Several controls were therefore performed to ensure that sulfatase activity was responsible for the observed phenotype. First, identical phenotypes were generated by injection of all four varieties of sulfatase tested (compare Fig. 3A with Fig. 1D). Second, as many sulfatase preparations are contaminated by glucuronidase activity, we injected type IX-A β-glucuronidase, which had no detectable sulfatase activity in an *in vitro* assay (see Materials and Methods). This enzyme elicited no abnormal phenotype (not shown). Third, to be sure that nonenzyme contaminants were not responsible for the phenotype, we injected heat-inactivated type H-5 sulfatase. This preparation had no detectable sulfatase activity *in vitro* and also elicited no abnormal phenotype when injected (Figs. 3B and 3C). Finally, the activity of type H-5 sulfatase was measured *in vitro* at the high pH (8.2; Gillespie, 1982) of the blastocoel fluid; it retained 98% of its activity.

Morphology of Sulfatase Phenotype

Axial tissues (e.g., neural tube, notochord, and somite) in control larvae are easily identifiable in whole-mount CSLM optical section (Fig. 4A). CSLM was therefore used to examine morphological details of the phenotype resulting from sulfatase injection. All experimental embryos observed in sagittal view at tailbud and tadpole stages (Figs. 4B–4F), including those displaying no externally identifiable structures (APDI = 0; Figs. 4E and 4F), had well-differentiated, vacuolated notochords and hollow neural tubes. In embryos

TABLE 1
Anteroposterior Deficiencies Index (APDI)

Grade	Description
5	Normal embryos (Fig. 1A)
4	Slight reduction of cranial structures (Fig. 1B)
3	More pronounced reduction of cranial structures including distinct reduction of the eyes and cement gland; mild truncation of anteroposterior axis (Fig. 1C)
2	Complete loss of eyes and cement gland; further cranial reduction; mild reduction of posterior axial structures (Fig. 1D)
1	Anterior defects similar to grade 2; truncation of posterior axial structures (Fig. 1E)
0	Complete loss of all externally visible axial structures; significant shortening of the anteroposterior axis (Fig. 1F)

Note. Embryos were injected at stage 9 with sulfatase, cultured to stage 40, and scored. Representative samples were used as standards for all further grading of phenotype severity. (Note: despite similar degrees of anterior reduction, some embryos of grade 1 had varying degrees reduction of the tail fin as compared to the sample shown in the figure.) The P0–P4 index generated by Yamaguchi and Shinagawa (1989) may be used for the quantification of anteroposterior phenotypes; however, we recommend the use of APDI presented here, as this index parallels the anteroposterior reduction component of the commonly used DAI (Kao and Elinison, 1988).

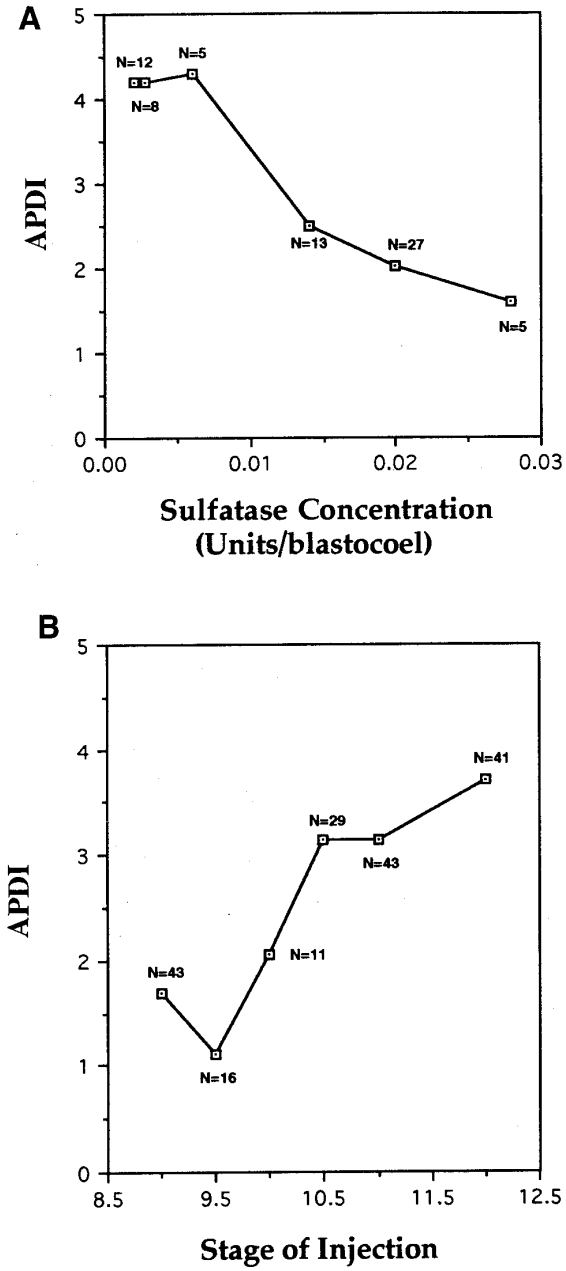

FIG. 2. The sulfatase-generated phenotype is dose dependent (A). Higher doses of enzyme result in more severe anterior–posterior truncations (n = 65 embryos from two independent experiments with two preparations of sulfatase). The phenotype is also time-dependent (B), with injections of 0.02 units/blastocoel at earlier stages resulting in more severe phenotypes than injections of the same dose at later stages (n = 183 embryos from two independent experiments using two preparations of sulfatase). The more pure type H-5 sulfatase was used for these experiments; identical phenotypes were generated with all varieties tested (see Fig. 3).

of grades 5–2 (Fig. 4A–4C), the neural tube retained its characteristic vesicular organization (Fig. 4D), although in more severely affected larvae, eyes and forebrain were diminished or absent. Evidence of muscle differentiation was also found in all grades of the sulfatase phenotype. Somite files were easily discernible in CSLM sections (Fig. 4C and data not shown). Even the most severely affected larvae (APDI = 0) twitched when prodded, indicating the presence of organized muscle and peripheral nervous system.

Sulfatase Inhibits Morphogenetic Movements of Gastrulation

Because of the recognized intimacy between gastrulation and anteroposterior patterning (cf., Nieuwkoop, 1985; Nieuwkoop *et al.*, 1985; Gerhart *et al.*, 1989; Slack *et al.*, 1992; Slack and Tannahill, 1992), the effects of sulfatase on embryos were examined during gastrulation. Mid-sagittal CSLM optical sections revealed that injection of sulfatase dramatically inhibited the morphogenetic movements of gastrulation, particularly the migration of the head mesoderm and the extension and inflation of the archenteron (Fig. 5).

During *Xenopus* gastrulation, cells of the involuted head mesoderm migrate as a well-defined mass along the roof of the blastocoel, finally merging with the involuted lateral and ventral mesoderm under the animal pole (Figs.

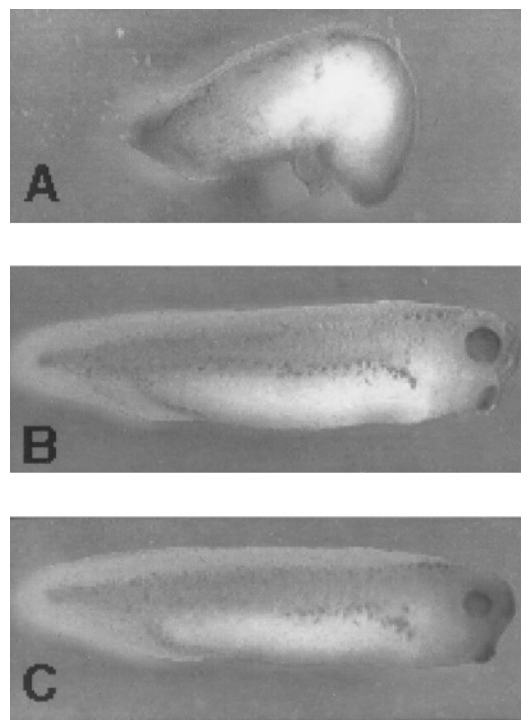

FIG. 3. Type H-5 sulfatase elicits anteroposterior truncation and ventral flexure when injected (0.02 units at stage 9) (A); this phenotype is identical to that elicited by type IV sulfatase (compare A with Figs. 1D and 1E). On the other hand, uninjected control (B) larvae are indistinguishible from those injected at stage 9 with 0.02 units of heat-inactivated H-5 sulfatase (C).

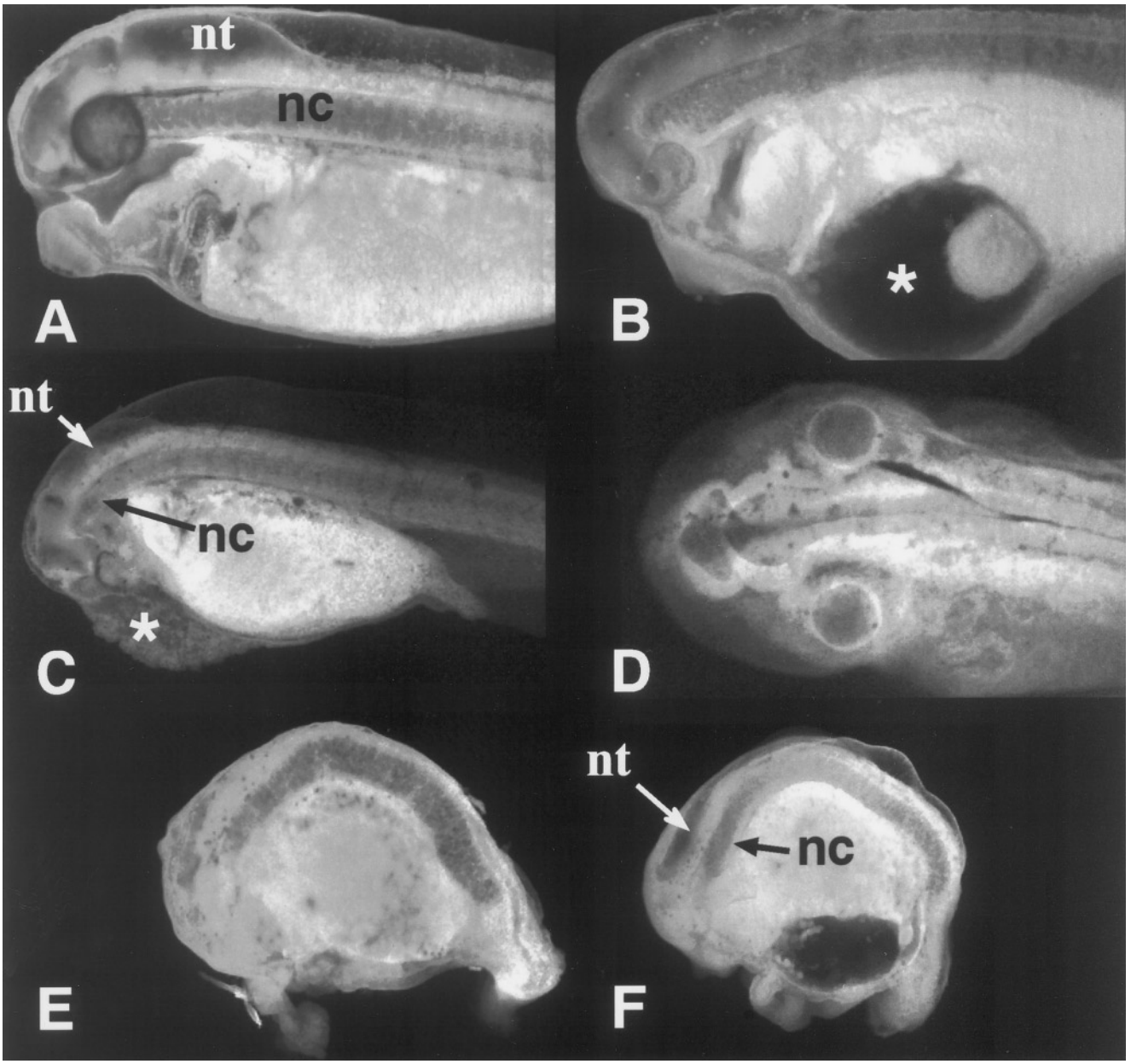

FIG. 4. Wholemount CSLM sections of larvae fixed at control stage 40. Control specimen (A; APDI = 5) shows well-differentiated notochord, heart, somites, and neural tube. Specimens shown in optical sagittal section in (B–F) were injected with type IV sulfatase at stage 9. Although deficient in the development of anterior cranial and axial structures, treated larvae retain a well-developed notochord, somites, and closed neural tube. Ventral flexure is restricted to anterior portions of the notochord and neural tube in less-severely affected individuals (B, APDI = 3; C, APDI = 2). In severe cases (E and F, APDI = 0), the entire anteroposterior axis is curved, and forebrain and eyes are absent; closed neural tube is present. Frontal section (D) of the individual shown in (C) reveals that the neural tube retains its characteristic vesicular organization; otocysts and kidney tubules are also evident. (nt, neural tube; nc, notochord) Persistent blastocoels are evident at tadpole stages as pericardial vesicles in specimens in B (*) and F. The remnants of similar vesicles which collapsed during larval development are visible in specimens in C (*) and E.

5A–5E; Keller, 1991). However, no such cell movement was observed during this period in embryos injected with sulfatase (Figs. 5F–5J); poleward migration of the head mesoderm in advance of the axial mesoderm was severely inhibited (Fig. 5, compare A and B with F and G). In many embryos, large gaps were observed between the dorsal mesoderm and the overlying ectoderm (Fig. 5F), suggesting that the head mesoderm was unable to attach to

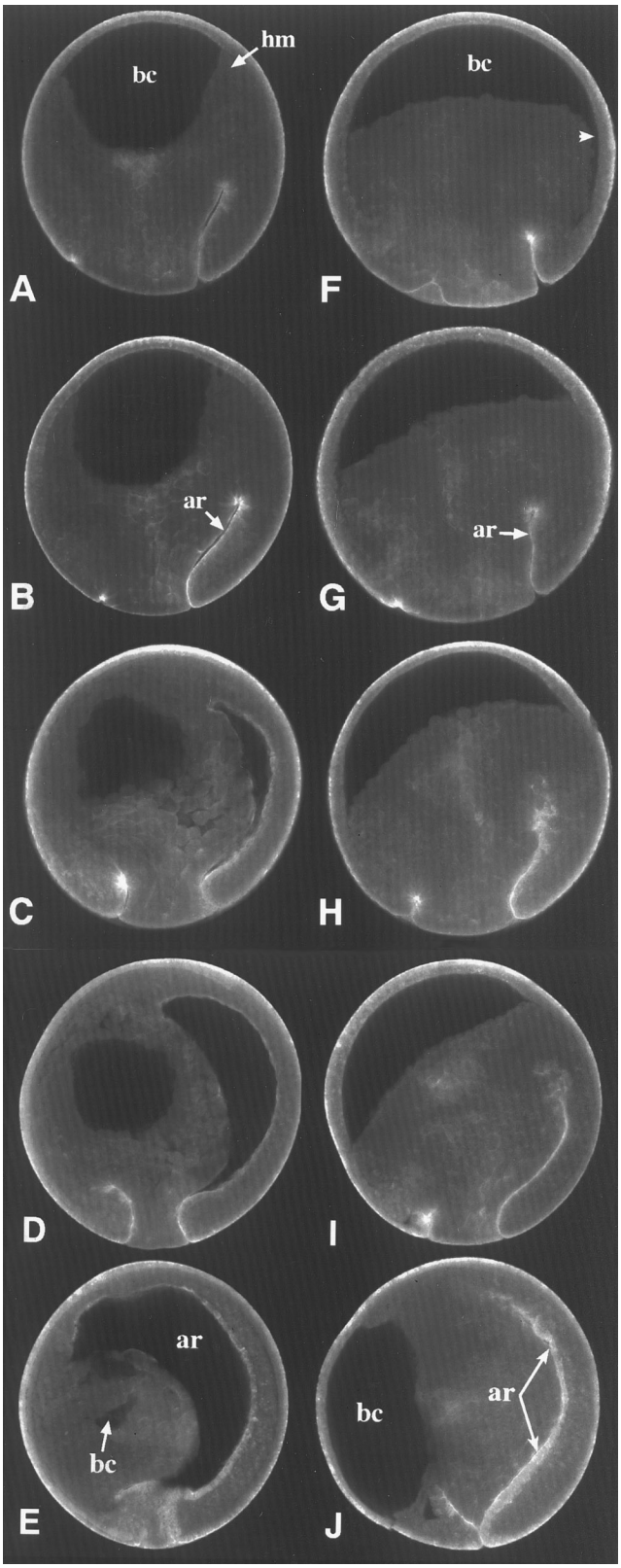

FIG. 5. Wholemount CSLM midsagittal sections of embryos fixed during gastrulation. All embryos are shown oriented with the dorsal blastopore lip in the lower right quadrant. Control specimens (A–E; fixed at stages 11, 11.5, 12, 12.5, and 13) show progressive involution of the marginal zone, migration of the head mesoderm (hm) across the roof of the blastocoel, expansion of the archenteron (ar), and eventual collapse of the blastocoel (bc). Sulfatase type IV-injected (0.02 units) specimens (F–J) fixed at equivalent stages likewise show progressive involution of the marginal zone and elongation, but not expansion, of the archenteron. The length of the archenteron in sulfatase-injected embryos is shorter than controls at all stages. Note also that the cells of the anterior axial mesoderm (nearer the blastocoel) appear less organized than at the posterior (nearer the blastopore). Migration of the head mesoderm in advance of the axial mesoderm does not occur (A–B, F–G); note the gap between head mesoderm and blastocoel roof in F (arrowhead). Note the persistent blastocoel, which is displaced ventrally as involution proceeds.

its migratory substrate, the blastocoel roof (Winklbauer, 1990).

The archenteron of *Xenopus* embryos normally inflates and extends in length as the blastocoel collapses during gastrulation (Figs. 5A–5E; Keller, 1991). In embryos injected with sulfatase however, we observed a complete failure of archenteron expansion (Figs. 5G–5J). As late as stage 13, when control archenterons have almost fully expanded (Fig. 5E), the archenterons of sulfatase injected embryos (Fig. 5J) were visible only as a narrow slit, a configuration reminiscent of the archenterons of control embryos at much earlier stages (Fig. 5A). Furthermore, the blastocoels of sulfatase-injected embryos (Figs. 5F–5J) did not deflate and were displaced ventrally, often persisting through larval development as large vesicles (see Figs. 4B and 4D). While this displacement was accompanied by an increase in distance between the leading edge of the mesodermal mantle and the dorsal blastopore lip, the amount of involution of the marginal zone (as defined by the length of the archenteron) in sulfatase-injected embryos was consistently less extensive than that of controls.

Sulfatase Inhibits Convergent Extension Movements in Dorsal Marginal Zone Explants

The fact that the archenteron does not extend and inflate properly in sulfatase-injected embryos suggests that the enzyme inhibits convergent extension of the axial mesoderm. However, as convergent extension of the involuted marginal zone drives blastopore closure (Shih and Keller, 1992), and the blastopore usually closes in sulfatase-injected embryos, it is possible that sulfatase does not affect the process directly, but inhibits archenteron extension at some other level. To determine directly whether or not sulfatase inhibits motility in the axial mesoderm, planar explants of the dorsal marginal zone (''Keller explants'') were isolated from early gastrula embryos and cultured in the presence or absence of sulfatase.

Convergent extension was compared in control and sulfatase-treated explants by measuring the amount of explant elongation occurring between stage 10+ and stage 17. While

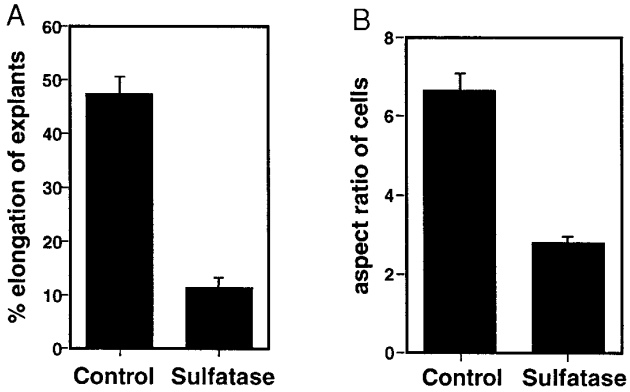

FIG. 6. Sulfatase inhibits convergent extension of dorsal marginal zone explants. Sulfatase severely reduces the extent of elongation of explants between stage 10+ and stage 17 (A). Control explants elongate by nearly 50% (47.1 ± 3.2, mean ± SEM; $n = 31$) during this interval, while mean elongation in sulfatase-treated explants is approximately 11% (11.3 ± 2.0, $n = 44$). This difference is extremely significant (Mann–Whitney test, $p < 0.0001$; Mann–Whitney U statistic, 43.00). These results show that sulfatase inhibits convergent extension. Aspect (length–width) ratios of mesoderm cells in control and sulfatase-treated explants at stage 17 (B). In control explants, mesoderm cells show a mean aspect ratio of 6.6 ± 0.4, revealing the degree of cell elongation that has taken place ($n = 30$ cells from three explants). In sulfatase-treated explants, the mean aspect ratio is 2.8 ± 0.2 ($n = 30$ cells from three explants). This difference is extremely significant (Mann–Whitney test, $p < 0.0001$; Mann–Whitney U statistic, 35.00), indicating that sulfatase inhibits elongation of mesoderm cells. This difference in cell aspect ratios is readily observable in high-magnification images (see Figs. 7C and 7D).

control explants show an average overall elongation of 47% during this interval, overall elongation is reduced to approximately 11% in sulfatase-treated embryos (Fig. 6A and Figs. 7A and 7B). Thus, sustained exposure to sulfatase dramatically inhibits convergent extension by the dorsal mesoderm.

Convergent extension involves a distinct sequence of cell behaviors: formation of bipolar protrusions, cellular elongation and alignment, and intercalation along the mediolateral axis (Shih and Keller, 1992; Domingo and Keller, 1995). Comparisons of mesodermal cells within control and sulfatase-treated explants show that mesodermal cells fail to elongate in the presence of sulfatase. Aspect (length-width) ratios of cells in control and sulfatase-treated explants were measured; for each treatment, a total of 30 cells from three explants were examined. Aspect ratios of elongated mesodermal cells from control explants are 6.6 on average. In contrast, aspect ratios of cells from the vegetalmost region of sulfatase-treated explants range around an average of 2.8 (Fig. 6B and Figs. 7C and 7D), indicating that cell elongation is strongly inhibited by sulfatase.

Convergent extension movements are most dramatic in the presumptive notochordal mesoderm. The inhibition of convergent extension may be the result of inhibited movement, or it could result from a failure to acquire dorsal character. To distinguish between these two alternatives, treated and untreated open-face Keller explants were stained with the notochord-specific antibody Tor70 (Figs. 7A and 7B, black arrows indicate staining). Over 77% (17/22) of treated explants expressed the Tor70 epitope, compared with 100% (18/18) of controls. In many cases, the amount of Tor70-positive tissue was reduced compared with controls. This reduction is very likely due to the requirement for short-range signals which themselves depend upon convergent extension; under conditions in which convergence and extension are blocked, notochord differentiation is greatly reduced (Shih and Keller, 1992; Domingo and Keller, 1995). Expression of Tor70 in most explants, however, indicates that sulfatase treatment does not prohibit the acquisition of dorsal character. Moreover, cement gland formation was frequently observed in the anterior ectoderm of both control and sulfatase-treated explants (Fig. 7, A&B). Since the cement gland is induced coordinately with the anterior neural ectoderm

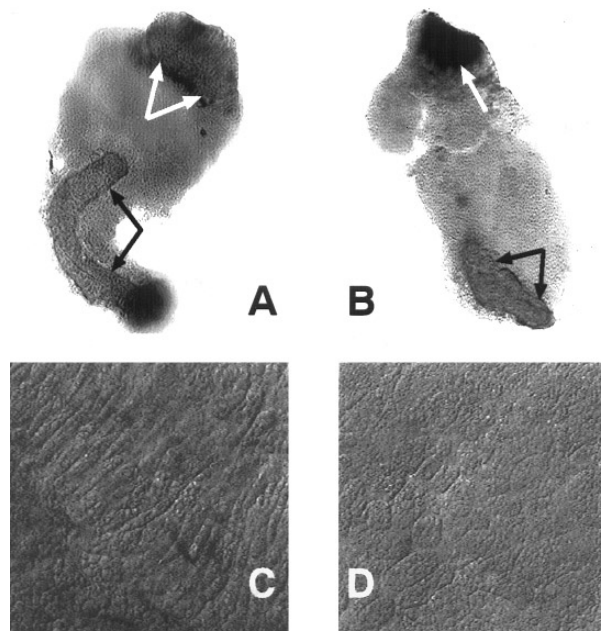

FIG. 7. Effects of sulfatase on planar explants of the dorsal marginal zone. Both control (A) and sulfatase-treated (B) explants express the notochord-specific antigen Tor70 (black arrows), indicating that sulfatase does not directly inhibit the mesoderm's ability to acquire dorsal axial character. White arrows indicate cement glands formed by the anterior ectoderm in both control (A) and sulfatase-treated (B) explants, indicating that the enzyme does not inhibit inductive interactions required for the planar anteroposterior patterning of anterior neural tissue. The reduction in the amount of notochord tissue formed in many sulfatase-treated explants is likely due to the absence of mediolateral intercalation behavior which is required for the propagation of short-range patterning signals. In untreated explants (C), cells are elongate, indicative of mediolateral intercalation behavior. No such behavior is observed in explants treated with sulfatase (D).

(Sive *et al.*, 1989), this finding suggests that the inductive signals responsible for anterior neural specification are not disrupted by sulfatase treatment.

The Sulfatase-Generated Phenotype Differs from UV-Generated Dorsoanterior Defects

Mitani (1989) observed retarded gastrulation in *Xenopus* embryos injected with heparin. Likewise, the polysulfonated compounds trypan blue and suramin retard gastrulation and result in disruption of the body axis (Gerhart *et al.*, 1989; Kao and Danilchik, 1991). Stage 40 tadpoles were therefore examined using CSLM to compare the sulfatase-generated phenotype with these other axially deficient phenotypes.

Heparin was injected into the blastocoels of embryos between stages 9 and 10. As previously reported (Mitani, 1989), this treatment produced drastic malformations (Fig. 8A), while similar doses of chondroitin sulfates elicited no such response (not shown). Sagittal CSLM sections confirmed the overall similarity of the sulfatase and heparin phenotypes (Fig. 8A, compare with Fig. 4C): a dose-dependent, progressive reduction of cranial and anteroposterior axial structures. Interestingly, a consistent characteristic of both phenotypes was a retention of notochord and closed neural tube following even the most severe treatments.

Trypan blue and suramin were also injected into the blastocoel at the onset of gastrulation. Like sulfatase and heparin, trypan blue and suramin elicited a dose-dependent loss of anteroposterior character. However, the latter two agents generated phenotypes accompanied by specific reduction of structures along the dorsoventral axis as well. In heparin- and sulfatase-injected embryos, the notochord extends near to the anterior limit of the embryo, regardless of the severity of the phenotype (Fig. 8A; Figs. 4C and 4F). In contrast, trypan blue-injected embryos (Fig. 8B) and suramin-injected embryos (not shown), despite the presence of such ventral–anterior structures as the cement gland, have no anterior notochord, neural tube, or somites, and even posterior trunk somites are fused and malformed (Fig. 8B). The trypan blue-generated phenotype is more reminiscent of that elicited by inhibition of the axis-specifying cortical–cytoplasmic rotation, for example, by irradiation of the vegetal cortex with UV light (Fig. 8C).

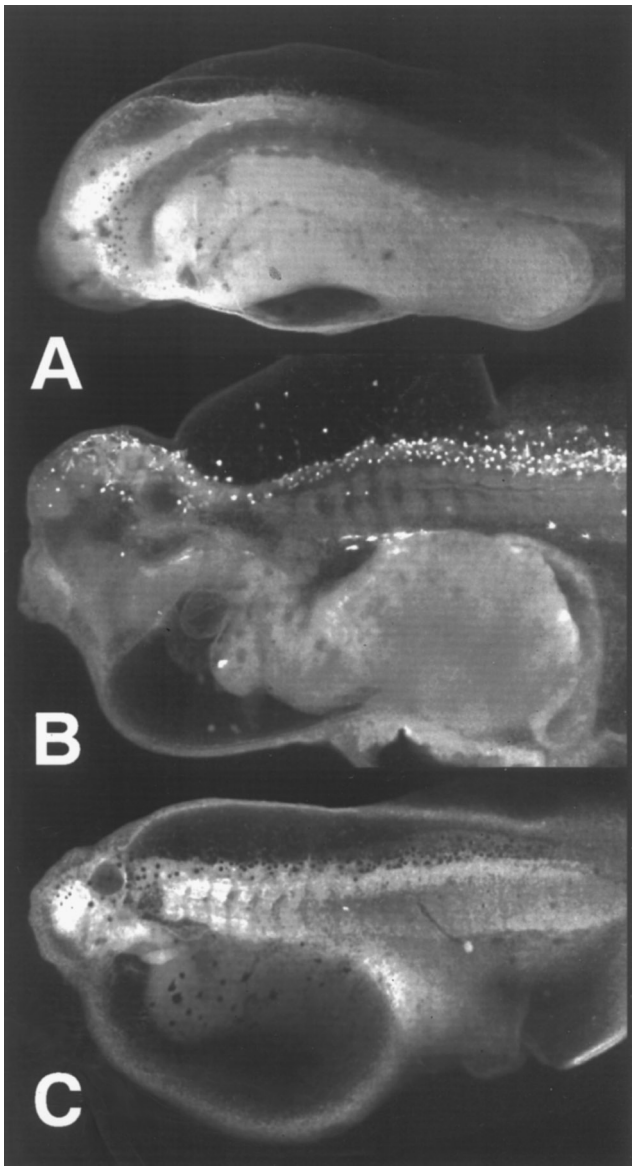

FIG. 8. At control stage 40 (see Fig. 3A), embryos injected during gastrulation with heparin (A) or trypan blue (B) or irradiated on the vegetal pole during the first cell cycle (C) exhibit marked reduction of anterior structures. Like sulfatase-injected embryos (see Fig. 3A), heparin injected embryos retain notochord and neural tube at the anterior-most end of the embryo. Trypan blue-injected embryos and UV-treated embryos, on the other hand, experience significant loss of dorsal structures (notochord, neural tube) as well as anterior (head) structures. The scattered bright spots in the trypan blue-treated larva are pigment granules, which sometimes become autofluorescent during whole-mount preparation.

DISCUSSION

Sulfatase Inhibits Gastrulation and Truncates the Anteroposterior Axis

Injection of sulfatase into the blastocoels of gastrulating *Xenopus* embryos strongly inhibited the morphogenetic movements of gastrulation and resulted in severe disruptions of anteroposterior pattern. We have used sulfatase teratogenesis as well as other axis-perturbing treatments to determine how morphogenetic movements at gastrulation contribute to the formation of both dorsoventral and anteroposterior axes. In this investigation, whole-mount confocal microscopy was used for rapid, high-resolution analysis of large numbers of specimens and also allowed the organization of cells and tissues at gastrulation to be resolved very finely in whole embryos not distorted by sectioning.

Sulfatase Inhibits Migration of the Head Mesoderm

The lack of poleward movement of the head mesoderm in advance of the axial mesoderm in sulfatase-injected embryos (Fig. 5) strongly suggests that sulfatase directly affects the migration of the head mesoderm, as this migration is independent of the other morphogenetic movements of the more posterior axial mesoderm (Winklbauer, 1990, Keller, 1991). The large gaps observed between the head mesoderm and its natural migratory substrate, the blastocoel roof (Winklbauer, 1990), indicate that migration may be blocked by a loss of affinity between these two tissues in the presence of sulfatase.

Migration of the prospective head mesoderm is mediated by a lattice of ECM fibers which cover the blastocoel roof (Winklbauer, 1990). Although RGD/fibronectin interactions appear to be important for guiding this motility, prospective head mesoderm cells are intrinsically motile and attach to the blastocoel roof in an RGD-independent manner (Winklbauer, 1990; Winklbauer and Nagel, 1991). The inhibition of head mesoderm migration by sulfatase suggests that a major component of this intrinsic attachment mechanism may be a sulfated macromolecule in the ECM of the blastocoel roof or at the surfaces of migrating mesoderm cells.

Regardless of the underlying biochemical mechanism, inhibition of head mesoderm migration likely contributes significantly to the loss of anterior structures in sulfatase-injected embryos, as the effects of inhibition of morphogenetic movement on larval pattern are likely to be compounded by consequential interruptions of signaling events. With gastrulation movements inhibited, many cells and tissues would not be properly positioned to send and/or receive signals. For example, vertical signals from the head mesoderm are required for eye formation in the overlying ectoderm (Ruiz i Altaba, 1992); in sulfatase-injected embryos, the head mesoderm does not migrate properly (Fig. 5), and eyes are often underdeveloped or absent.

Sulfatase Inhibits Expansion and Elongation of the Archenteron

In embryos injected with sulfatase, both the elongation and expansion of the archenteron are significantly retarded. The primary forces driving archenteron elongation are the migration of the head mesoderm and the convergent extension of the axial mesoderm. As both of these processes are disrupted by sulfatase, the failure of archenteron elongation is not surprising.

More interesting is the failure of archenteron expansion. The mechanism underlying expansion of the archenteron is poorly understood, so it remains unclear at this point whether this failure represents a dependence of archenteron expansion upon the morphogenetic movements of the adjacent mesoderm or a direct effect of sulfatase on the respreading of bottle cells, an independent morphogenetic process (Keller, 1981; Hardin and Keller, 1988).

Beginning approximately midway through gastrulation and continuing into early neurula stages, the bottle cells change from a flask shape to a cuboidal or squamous shape, resulting in a dramatic expansion in surface area of the bottle cell epithelium. The respread bottle cells give rise to the anterior archenteron and the archenteron walls (Hardin and Keller, 1988; Keller, 1981). As the archenterons of sulfatase-injected embryos at late gastrula stages (Fig. 5J) resemble the archenterons of control embryos prior to bottle cell respreading (Fig. 5A), our data seem to indicate that sulfatase inhibits this process directly. Furthermore, as respreading of the bottle cell epithelium may involve active migration on the part of the bottle cells (Hardin and Keller, 1988; Keller, 1981) and sulfatase inhibits the migration of the head mesoderm cells, the failure of archenteron expansion in sulfatase injected embryos also argues that sulfatase may disrupt active motility of the bottle cells that may be required for respreading. These possibilities are under investigation.

In summary, our data suggest that expansion of the archenteron may be an independent morphogenetic event which is required for the completion of anteroposterior patterning of the *Xenopus* embryo. As such, the inhibition of three morphogenetic processes—archenteron expansion, head mesoderm migration, and convergent extension—contributes to the phenotype of anteroposterior truncation seen in embryos injected with sulfatase.

Inhibition of Morphogenetic Movements Accounts for the Anteroposterior Truncation Induced by Sulfatase

As the extent of morphogenetic movements during gastrulation is directly correlated with the extent of anteroposterior patterning (Gerhart *et al.*, 1989; Slack *et al.*, 1992; Slack and Tannahill, 1992), our data indicate that the phenotype generated by sulfatase may be a direct result of disrupted morphogenetic movements during gastrulation. The observed inhibition of morphogenetic movements during gastrulation in whole embryos is consistent with this hypothesis. Furthermore, the presence of such dorsal axial structures as vacuolated notochord and closed neural tube in sulfatase-injected embryos at all grades of severity suggests that sulfatase does not eliminate the tissue's ability to acquire dorsal axial character. Likewise, sulfatase inhibited convergent extension of dorsal marginal zone explants without eliminating the expression of the notochord-specific Tor70 epitope, although the amount of notochord tissue was reduced. This result indicates that sulfatase does not directly inhibit the embryos' ability to acquire dorsal axial character, but rather the enzyme disrupts notochord formation by inhibiting convergent extension movements and therefore the propagation of the short-range signals required for differentiation along the anterior-to-posterior extent of the notochord (Shih and Keller, 1992). Likewise, the appearance of cement glands in sulfatase-treated explants suggests that this treatment does not inactivate anterior inducing signals responsible for the coordinated specification of cement gland and anterior neural ectoderm.

Similarly, mechanical blockage of convergent extension movements also inhibits proper completion of the anterior to posterior differentiation of notochord and somite in dorsal marginal zone explants, although notochord- and muscle-specific epitopes are expressed in these explants (Shih and Keller, 1992; Domingo and Keller, 1995). Therefore, in mechanically restrained explants as well as whole embryos and explants treated with sulfatase, convergent extension is inhibited, yet specification of only the anteroposterior axis appears disrupted. Taken together, these results suggest that dorsoventral patterning can be experimentally uncoupled from anteroposterior patterning during gastrulation by inhibition of morphogenetic movements.

A direct inhibition of morphogenetic movement can then account for the observed anteroposterior truncation in sulfatase-treated embryos. Injection into the blastocoel will preferentially expose the anterior (earliest involuting) mesoderm to sulfatase, resulting in only anterior defects at low doses, while higher doses affect progressively more posterior tissue. However, at most doses, posterior mesoderm is not severely affected, and convergent extension in these areas can drive blastopore closure (Shih and Keller, 1992). This conclusion is consistent with our finding that the highest doses of sulfatase inhibited blastopore closure. This conclusion is also supported by the observation that the cells composing the anterior archenteron of sulfatase-injected embryos tend to be jumbled and disorganized, while the organization of the cells in the posterior archenteron of the same embryo appears normal (Figs. 5H–5J).

The Anteroposterior Truncation Phenotype Generated by Sulfatase Is Distinctly Different from Recognized Dorsoanterior Truncation Phenotypes

Midsagittal CSLM sections of experimental embryos revealed that the phenotype generated by sulfatase differs significantly from that generated by trypan blue and UV. As previously described (Malacinski *et al.,* 1977; Greenhouse and Hamburgh, 1968; Waddington and Perry, 1956), phenotypes generated by the latter two agents are characterized by anteroposterior truncation, incomplete closure of the neural tube, reduction and fragmentation of the notochord, and fusion of the somite pairs; in the most severe cases, these dorsal axial structures are not found at all. Hence, these phenotypes are classed as dorsoanterior reductions (see Table 2) and are quantified by the DorsoAnterior Index of Kao and Elinson (1988).

The sulfatase-generated phenotype, on the other hand, despite severe anteroposterior truncation, retains all levels of dorsoventral character (closed neural tube, vacuolated notochord, and organized muscle) in all cases, making it very reminiscent of the heparin-generated phenotype (Mitani, 1989). Although the heparin-induced phenotype has been previously considered to be a dorsoanterior reduction (Cardellini *et al.,* 1995), we feel that these phenotypes are more accurately defined as anteroposterior reductions. These phenotypes are also similar to that generated by treatment with lithium after the midblastula transition (Yamaguchi and Shinagawa, 1988). All three of these treatments truncate the anteroposterior axis without eliminating dorsoventral pattern; for this reason, these phenotypes cannot be accurately quantified by the DorsoAnterior Index. While the P0–P4 scale designed by Yamaguchi and Shinagawa (1988) can be used to quantify anteroposterior reduction phenotypes, we have generated an index (the APDI) with six grades which corresponds to the anteroposterior reduction component of the DAI.

TABLE 2

Classification of Dorsoanterior and Anteroposterior Phenotypes

Treatment	Resulting phenotype
Type H-1 sulfatase	APDI[a]
Type H-5 sulfatase	APDI
Type VIII sulfatase	APDI
Type IV sulfatase	APDI
Heat-inactivated H-5 sulfatase	—[b]
Type IX-A β-glucuronidase	—
Bovine serum albumin	—
Heparin	APDI
Heparan sulfate	APDI
Chondroitin-3-sulfate	—
Trypan Blue	DAI[c]
Suramin	DAI
Ultraviolet irradiation[d]	DAI

Note. Embryos were injected at stage 9 with the compounds listed, cultured to stage 40, and then examined for axial defects.

[a] APDI: larval morphology characterized by anteroposterior reduction phenotype (e.g., via sulfatase injection; see Table I).

[b] —: no axial deficiencies.

[c] DAI: larval morphology characterized by dorsoanterior reduction phenotype (see Kao and Elison, 1988).

[d] Treatment prior to cortical rotation.

Dorsoanterior versus Anteroposterior Truncations: Separation of Distinct Components of the Axis-Generating Machinery

The two classes of axially deficient embryos appear to result from disparate mechanisms of teratogenesis and reveal two largely separable components of the axis-generating machinery of the embryo. In the well-characterized dorsoanterior reduction phenotype generated by UV irradiation, the loss of axial character along the dorsoventral axis is a direct result of inhibition of dorsal mesoderm specification (Gerhart *et al.,* 1989). The disruption of morphogenetic gastrulation movements—which will account for loss of axial character along the anteroposterior axis—is a secondary effect, resulting from the absence of dorsal mesoderm. This model accounts for the observed loss of character along both anteroposterior and dorsoventral axes.

The striking similarity between the UV phenotype and the trypan blue-induced phenotype (Fig. 8) suggests that inhibition of dorsal mesoderm specification or differentiation may also be the primary defect in suramin- and trypan

blue-injected dorsoanteriorly deficient embryos. This hypothesis is supported by the finding that treatment of dorsal blastopore lips with suramin inhibits notochord formation (Grunz, 1993). Because injection of suramin or trypan blue as late as mid-gastrula stages results in severe dorsoanterior truncation (data not shown; Gerhart *et al.*, 1989), these agents may be interfering with signals which modify the dorsoventral character of the mesoderm during gastrula stages (e.g., member(s) of the Wnt family, Christian and Moon, 1993; noggin, Smith and Harland, 1992; chordin, Sasai *et al.*, 1994; or BMP-4, Dale *et al.*, 1992). Thus, a failure to acquire dorsal character seems to be the underlying mechanism of all dorsoanterior reduction phenotypes.

Conversely, we propose that the anteroposterior phenotypes, such as that produced by injection of sulfatase at gastrula stages, are largely independent of dorsoventral patterning and are attributable primarily to the blockage of morphogenetic movements during gastrulation compounded by secondary disruptions of inductive events (see above). Careful examination of novel axially deficient phenotypes may indicate which process is being affected by the experimental manipulation. We propose that a distinction can be made between dorsoanterior phenotypes and anteroposterior phenotypes and that this distinction is particularly important to consider when relating morphogenetic movements and inductive interactions during early development to later embryonic patterning.

ACKNOWLEDGMENTS

The authors thank B. Brown, J. Christian, K. Larkin, and P. Vize for their helpful comments. J.B.W. would like to thank Alice Kagi, an inspiring teacher. The authors also acknowledge Dick Dale for his enormous contribution. M.V.D. was supported by NSF DCB-8916614, March of Dimes BOC 5-721, and a project grant from Wesleyan University to M.V.D. J.B.W. was supported by an Undergraduate Research Fellowship from Wesleyan University's Hughes Program in the Life Sciences and at UT Austin by Texas Advanced Research Program 187 to Peter Vize. Work in the laboratory of A.K.S. was supported by NSF DCB-9118746 and by Texas Advanced Research Program 131.

REFERENCES

Brickman, M. C., and Gerhart, J. C. (1994). Heparitinase inhibition of mesoderm induction and gastrulation in *Xenopus laevis* embryos. *Dev. Biol.* **164,** 484–501.

Cardellini, P., Polo, C., and Coral, S. (1994). Suramin and heparin: Aspecific inhibitors of mesoderm induction in the *Xenopus* embryo. *Mech. Dev.* **45,** 73–87.

Christian, J., and Moon, R. (1993). Interactions between Xwnt-8 and the spemann organizer signalling pathways generate dorsoventral pattern in the embryonic mesoderm of Xenopus. *Genes Dev.* **7,** 13–28.

Dale, L., Howes, G., Price, B. J. M., and Smith, J. C. (1992). Bone morphogenetic protein 4: A ventralizing factor in early *Xenopus* development. *Development* **115,** 573–585.

Danilchik, M. V. (1986). Effect of trypan blue on mesodermal cell migration during gastrulation in *Xenopus laevis. J. Cell Biol.* **103,** 244a. [Abstr. 912]

Dent, J. A., and Klymkowsky, M. W. (1989). Whole-mount analysis of cytoskeletal reorganization and function during oogenesis and early embryogenesis in *Xenopus. In* ''The Cell Biology of Fertilization'' (H. Schatten and G. Schatten, eds.), pp. 63–103. Academic Press, San Diego.

Dodgson, K. S., and Spencer, S. (1957). Assay of sulfatases. *Methods Bioc. Anal.* **4,** 211–255.

Domingo, C., and Keller, R. (1995). Induction of notochord cell intercalation behavior and differentiation by progressive signals in the gastrula of *Xenopus* laevis. *Development* **121,** 3311–3321.

Gerhart, J., Danilchik, M., Doniach, T., Roberts, S., Rowning, B., and Stewart, R. (1989). Cortical rotation of the Xenopus egg: Consequences for the anteroposterior pattern of embryonic dorsal development. *Development* (Suppl.), 37–51.

Gillespie, J. I. (1983). The distribution of small ions during the early development of *Xenopus laevis* and *Ambystoma mexicanum* embryos. *J. Physiol.* **344,** 359–377.

Greenhouse, G., and Hamburgh, M. (1968). Analysis of trypan blue induced teratogenesis in *Rana pipiens* embryos. *Teratology* **1,** 61–74.

Grunz, H. (1993). The dorsalization of spemann's organizer takes place during gastrulation in *Xenopus laevis* embryos. *Dev. Growth. Differ.* **35,** 25–32.

Hardin, J., and Keller, R. (1988). The behaviour and function of the bottle cells during gastrulation of Xenopus laevis. *Development* **103,** 211–230.

Harland, R. (1991). In situ hybridization: an improved method for Xenopus embryos. *In* ''Methods in Cell Biology'' (B. K. Kay and H. B. Peng, Eds.), Vol. 36, pp. 685–695. Academic Press, San Diego.

Hemmati-Brivanlou, A., and Harland, R. M. (1989). Expression of an engrailed-related protein is induced in anterior neural ectoderm of early *Xenopus* embryos. *Development* **106,** 611–617.

Itoh, K., and Sokol, S. (1994). Heparan sulate proteoglycans are required for mesoderm formation in *Xenopus* embryos. *Development* **120,** 2703–2711.

Kao, K. R., and Danilchik, M. V. (1991). Generation of body plan phenotypes in early embryogenesis. *In* ''Methods in Cell Biology'' (B. K. Kay and H. B. Peng, Eds.), Vol. 36, pp. 271–284. Academic Press, San Diego.

Kao, K. R., and Elinson, R. P. (1988). The entire mesodermal mantle acts as Spemann's organizer in dorsoanterior enhanced *Xenopus laevis* embryos. *Dev. Biol.* **127,** 64–77.

Keller, R. E. (1981). An experimental analysis of the role of the bottle cells and deep marginal zone in gastrulation of Xenopus laevis. *J. Exp. Zool.* **216,** 81–101.

Keller, R., and Danilchik, M. (1988). Regional expression, pattern and timing of convergence and extension during gastrulation of *Xenopus laevis. Development* **103,** 193–209.

Keller, R., and Tibbetts, P. (1989). Mediolateral cell intercalation in the dorsal, axial mesoderm of *Xenopus laevis. Dev. Biol.* **131,** 539–549.

Keller, R. (1991). Early embryonic development of *Xenopus laevis. In* ''Methods in Cell Biology'' (B. K. Kay and H. B. Peng, Eds.), Vol. 36, pp. 61–113. Academic Press, San Diego.

Malacinski, G. M., Brothers, A. J., and Chung, H-M. (1977). Destruction of components of the neural induction system of the amphibian egg with ultraviolet irradiation. *Dev. Biol.* **56,** 34–39.

Mitani, S. (1989). Retarded gastrulation and altered subsequent development of neural tissues in heparin-injected *Xenopus* embryos. *Development* **107,** 423–435.

Moore, S. M., Keller, R. E., and Koehl, M. A. R. (1995). The dorsal involuting marginal zone stiffens anisotropically during its convergent extension in the gastrula of *Xenopus laevis. Development* **121,** 3131–3140.

Nieuwkoop, P. D. (1985). Inductive interactions in early amphibian development and their general nature. *J. Embryol. Exp. Morph.* **89**(Suppl.), 333–347.

Nieuwkoop, P. D., Johnen, A. G., and Albers, B. (1985). ''The Epigenetic Nature of Early Chordate Development: Inductive Interaction and Competence.'' Cambridge University Press, Cambridge.

Nieuwkoop, P. D., and Faber, J. (1994). ''Normal Table of *Xenopus laevis* (Daudin).'' Garland Publishing, New York.

Peng, H. B. (1991). Solutions and protocols. *In* ''Methods in Cell Biology'' (B. K. Kay and H. B. Peng, Eds.), Vol. 36, pp. 657–662. Academic Press, San Diego.

Ruiz i Altaba, A. (1992). Planar and vertical signals in the induction and patterning of the *Xenopus nervous* system. *Development* **116,** 67–80.

Sassai, Y., Lu., B., Steinbresser, H., Geissert, D., Gont, L. K., and De Reobertis, E. M. (1994). *Xenopus* Chordin: A novel dorsalizing factor activated by organizer-specific homeobox genes. *Cell* **79,** 779–790.

Sater, A., Steinhardt, R. A., and Keller, R. (1993). Induction of neuronal differentiation by planar signals in *Xenopus* embryos. *Dev. Dyn.* **197,** 268–280.

Shih, J., and Keller, R. (1992). Patterns of cell motility in the organizer and dorsal mesoderm of *Xenopus laevis. Development* **116,** 915–930.

Sive, H., Hattori, K., and Weintraub, H. (1989). Progressive determination during formation of the anteroposterior axis in *Xenopus laevis. Cell* **58,** 171–180.

Slack, J. M. W., Isaacs, H. V., Johnson, G. E., Lettice, L. A., Tannahill, D., and Thompson, J. (1992). Specification of the body plan during *Xenopus* gastrulation: Dorsoventral and anteroposterior patterning of the mesoderm. *Development* (Suppl.), 143–149.

Slack, J. M. W., and Tannahill, D. (1992). Mechanisms of anteroposterior axis specification in vertebrates—Lessons from amphibians. *Development* **114,** 285–302.

Smith, W. C., and Harland, R. M. (1992). Expression cloning of noggin, a new dorsalizing factor localized to the Spemann organizer in *Xenopus* embryos. *Cell* **70,** 829–840.

Waddington, C. H., and Perry, M. M. (1956). Teratogenic effects of trypan blue on amphibian embryos. *J. Embryol. Exp. Morphol.* **4,** 110–119.

Winklbauer, R. (1990). Mesodermal cell migration during *Xenopus* gastrulation. *Dev. Biol.* **142,** 155–168.

Winklbauer, R., and Nagel, M. (1991). Directional mesoderm migration in the *Xenopus* gastrula. *Dev. Biol.* **148,** 573–589.

Yamaguchi, Y., and Shinagawa, A. (1989). Marked alteration at midblastula transition in the effect of lithium on formation of the larval body plan of *Xenopus laevis. Dev. Growth Differ.* **31,** 531–541.

Received for publication April 11, 1996
Accepted March 21, 1997